J Mar Sci Technol (2015) 20:487–504
DOI 10.1007/s00773-014-0301-2

ORIGINAL ARTICLE

Positioning capability of anchor handling vessels in deep water during anchor deployment

Xiaopeng Wu · Giri Raja Sekhar Gunnu · Torgeir Moan

Received: 8 March 2014 / Accepted: 29 November 2014 / Published online: 3 January 2015

Abstract The aim of this paper is to study anchor handling vessel (AHV) thrust capacity during anchor deployment, especially in a deep water situation when high external forces are expected. The focus is on obtaining realistic external forces and evaluating the positioning capability of an AHV. Wind, wave and current loads on the AHV are considered. Current load on the mooring line, which is usually excluded in practice, is included in the model as well. The thrust utilisation plot, a concept widely used in the Dynamic Positioning system, is proposed to illustrate the positioning capability of an AHV. The Bourbon Dolphin accident was investigated as a case study using the proposed model and methodology. First, load analysis was performed. The results indicated the importance of applying a reasonable current profile and taking the mooring line effect into account. Then, thrust utilisation plots for normal and accident conditions were compared. The comparison showed that the Bourbon Dolphin might have been in the most unfavourable weather direction in terms of position capability during the accident event. Finally, the effect of mooring line configuration was studied. The results signified that a very long mooring line might challenge the propeller thrust capacity and the propeller thrust loss due to lateral thrust usage needs to be considered. Such an analysis and documentation prior to the commencement of the operation can be used for defining vessel specific limitations and selecting the proper vessel for a specific task.

Keywords Anchor handling · Drifting · Positioning capability · Thrust utilisation plot · Current profile

1 Introduction

Anchor handling operation (AHO) is considered to be one of the potentially most hazardous and demanding marine operations in the offshore industry. Characterised by bad weather, long working hours and high-tension load, AHOs are inherently dangerous, especially in a deep water situation when high external forces are expected. Meanwhile, the AHOs have a significant economical influence on the offshore projects. According to Saasen et al. [1], AHOs may carry 10–20 % of the total well exploitation cost because hiring the anchor handling vessel (AHV) is expensive. Considering daily hire rates on the spot market, costs may be as high as 900,000 Norwegian krones. The safety and economic factors make the AHO even more important.

The planning and execution of AHO are of significance. Skilled crew and well-designed vessels are needed to fulfil the tasks. Any miscalculation or misjudgment prior or during the operation might lead to project delay and economic loss. In the extreme cases, miscalculation or misjudgment can lead to casualties. The risk associated with AHO was recently demonstrated by the Bourbon Dolphin accident in 2007 [2], which claimed eight lives. The vessel lost stability due to a series of complex circumstances during the job in the Rosebank oilfield. Another loss of AHV was reported in 2003 [3]. The Danish vessel "Stevns Power" lost stability during an anchor retrieval operation. Eleven people died in this accident. Both of the above

X. Wu (✉) · G. R. S. Gunnu · T. Moan
Centre for Ships and Ocean Structures (CeSOS), NTNU, Trondheim, Norway
e-mail: xiaopeng.wu@ntnu.no

G. R. S. Gunnu
Global Maritime AS, Stavanger, Norway

accidents were characterised by a short time window before the vessel capsized. Despite only two instances of capsizing AHVs in the past decade, the consequences are fatal. How to enhance the safety level of the AHOs remains a challenging topic for all relevant societies, companies and research institutes.

To date, the AHVs are still treated as normal supply vessels with respect to stability requirements. These requirements are not sufficient to address the complexity and the forces involved in the AHOs. Due to huge mooring loads and the constraint of the mooring line hanging over the stern, these vessels face a high risk of capsizing. Taking the mooring line effect into account is indeed necessary, and how to modify the existing rules and regulations or establish related criteria would be of interest. For example, Gunnu and Moan [4] proposed a modified stability criterion for AHVs in the operational phase, in which the initial heel of the vessel due to mooring load was considered.

Situation awareness can also help to reduce the risk level. The AHOs are usually under tight schedules. The desire to be on schedule could hamper the safety of the operations. Both of the two notable accidents mentioned had shown such a desire, which might be one cause of the misjudgement. The master on board needs condensed and easily understood information about the situation to make good decisions. Hukkelås [5] proposed a new anchor handling concept to increase the safety. Situation awareness is the key in this concept. The stability margin is calculated and visualised in real time, which provides the master much more information about the vessel stability than before. Therefore, the master has a higher chance of making rational decisions.

Because the AHO is a series of complex activities, it would be difficult to secure safety for just one or two measures. More risk-mitigation measures need to be developed and added into the overall picture of the operation. For example, the risk influencing factors associated with the Bourbon Dolphin accident have been addressed by Gunnu et al. [6]. The considerable vessel drift during the AHO is considered as an initiating event for this accident. The track plot for the Bourbon Dolphin before the accident is shown in Fig. 1. The red line in the figure indicates the track for the Bourbon Dolphin from the commencement of deploying mooring line no. 2 until the accident. It is shown that in the early stage the vessel was capable of following the planned path of the mooring line. However, the vessel began to drift gradually and continually, paying out more mooring line under unfavourable weather conditions. The blue line shows the track for another AHV at the site that tried to help the Bourbon Dolphin. The black arrows are added by the authors to indicate the mooring line orientation and weather direction. This information will be explained further in the paper.

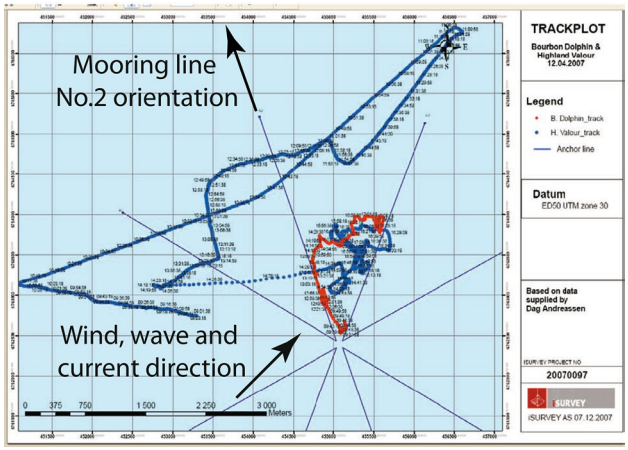

Fig. 1 Track plot of the Bourbon Dolphin (*red line*) [2] (colour figure online)

Extensive drift for the AHV can be unfavourable and even hazardous. First, extensive drift compromises the functionality requirement of the vessel, which is to deliver the mooring line in the desired position. Moreover, extensive drift could compromise safety, which requires maintaining the stability of the vessel. When the master tries to regain the correct course from an extensive drifting condition, it will be very tempting for him to manoeuvre the vessel in a way that develops a large angle of attack (β, the angle between the mooring line and the ship centre line). A plan view of an AHV drifting off course and trying to get back to course is illustrated in Fig. 2. A larger angle of attack means a larger lever arm for the vertical component of the morning load and a larger transverse component of the morning load. The combination of these two leads to larger overturning moment on the vessel which can be hazardous from the vessel stability perspective. Therefore, it is crucial to prevent significant drift and a large angle of attack during AHO, especially in deep water operations due to higher external loads and mooring loads are expected in these operations.

The hazardous conditions related to vessel stability can be averted by means of taking proper decisions and by executing appropriate ship handling skills. In practice, according to the opinions expressed by AHV masters, the hazardous misaligned mooring load can be handled either

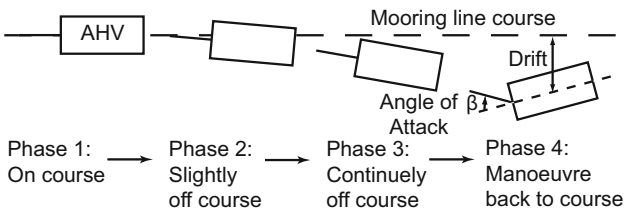

Fig. 2 Off course

by means of reducing the angle of attack (the vessel heading is adjusted such that the misaligned mooring line is in line with vessel heading) or by reducing the mooring line tension. Usually, the master will give priority to the former one because this is an optimised solution at this phase to fulfil both functional and safety requirements. This is achieved by correcting AHV heading first so that the angle of attack will be small and the AHV will be in the phase 1 condition in Fig. 2 in a normal operation. However, lack of ship handing capacity (poor ship positioning capability), or poor ship handling skills (incorrect maneuvering action), or a combination of these two can lead to an extensive drift condition. This might subsequently lead to the phase 4 condition in Fig. 2 when the master try to regain the correct course. The safety, i.e. the stability of the AHV, will then become more important at this stage and the functionality requirement shall become less significant. In such a hazardous situation, the master might reduce the propulsion thrust to reduce the mooring line tension, or even release the mooring line (by activating emergency releasing or quick releasing system) so that the AHV capsize situation can be avoided.

To prevent the unfavourable consequence or hazardous situation caused by the extensive drift, it is essential to have an awareness on the vessel positioning capability. When selecting the proper vessel for an anchor handling task, however, the major concern is normally put on available bollard pull (the maximum pulling force that a vessel can exert on another vessel or object), winch capacity and deck storage space. It seems that the positioning capability is not treated with enough care. The possible consequence is demonstrated in the Bourbon Dolphin accident. If the positioning capability of the vessel was well understood before the operation commenced, the master might have decided to delay the operation until more favourable weather condition came. As a result, there is a need to study the positioning capability of the AHV during anchor deployment. A method needs to be developed to evaluate the positioning capability of the AHV to help all parties involved in the operation gain a better picture before the operation commences. Useful information about the vessel position capability can then be generated, and operation limitation can be obtained. On the basis of this information, critical scenarios can be established as an input to simulator training.

The aim of this paper is to establish and use a detailed numerical model to study AHO during anchor deployment. Focus is put on obtaining realistic external forces on the vessel and evaluating the positioning capability of an AHV. The thrust utilisation plot is proposed to demonstrate the AHV positioning capability. The remainder of the article is organised as follows. The next section gives a detailed description of the main scenario and the flow chart in this work. In Sect. 3, the numerical methodology involved are addressed. Then the Bourbon Dolphin is studied as a case. Analysis and results are presented in Sect. 4. Finally, some conclusions are drawn in Sect. 5.

2 Scenario description and flow chart

There are various types of AHOs, depending on location, equipment on vessel, mooring methods, etc. The practical aspects of AHOs are discussed extensively by Ritchie [7] and Gibson [8]. Among different practical means, one basic method uses the permanent chaser pendant (PCP) system which mainly includes a wire hanging permanently attached to the rig used for chasing out anchors, and a ring fitted over the anchor line connected to the pendant wire. The mooring line can be handled by the rig or by the anchor handling vessel through this system. This method is the least complex method in anchor handling.

Within a PCP anchor handling operation, one common scenario is that the AHV delivers the mooring line to the desired location while the rig pays out the mooring line. This basic but important scenario is illustrated in Fig. 3. During this phase, the vessel is subjected to environmental forces coming from wind, swell, wave and current. In addition, the vessel carries mooring load coming from the mooring line. The magnitude and orientation of the mooring load vary during the whole operation, based on the total pay-out length of the line, the shape of the line, the speed of the vessel and the environmental conditions. The more mooring line has been paid out, the higher the force that will be exerted on the vessel. The vessel should have sufficient bollard pull to counteract the mooring load and provide propulsion forward. To maintain the desired heading, the lateral forces should be balanced by the thrusters and azimuth.

The Bourbon accident happened in this scenario, which makes the scenario very typical and worth studying. According to the accident report, there were several deficiencies in the rig move procedure relevant to this scenario. First, the current load on the mooring line was not included when estimating the static loads on the vessel, resulting in the underestimation of the static loads on the vessel and might be leading to the considerable drift. In fact, the vertical current profile, as will be discussed in this paper,

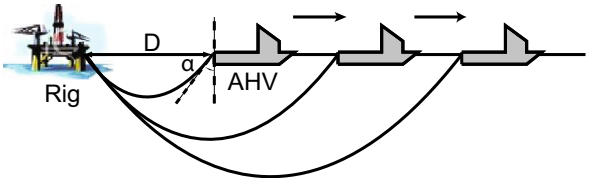

Fig. 3 Typical anchor handling operation

has a significant influence on the mooring line loads. Second, when the side thrusts are running at full capacity, the vessel bollard pull would show a significant drop. The vessel could then be pulled backward by the huge mooring load and could not finish the task. To overcome the deficiencies mentioned above, the thrust utilisation plot which is a concept in the Dynamic Positioning (DP) system, is introduced in this study.

DP capability analysis is an important part in the design of DP vessels as well as DP-related operations. The results are usually presented in the form of capability plots, which are polar plots indicating the limiting mean wind speed envelope for the vessel. More details about the basics of DP capability plots can be found in [9]. When the design sea state is predefined, the DP capability can be presented by means of a thrust utilisation plot, which shows the ratio envelope between the required thrust and the maximum available thrust [10]. The purpose of the DP capability plots and the thrust utilisation plots is to determine the position keeping ability of the vessel under various environmental conditions. In the guidelines for the safe operation of DP vessels, it is mentioned that the DP capability plots should be used in the risk assessment process to determine the safe working limits at offshore installations (see [11]). Because in AHO, the operation weather limit is usually predefined, the thrust utilisation plot is more suitable in this study.

The DP function, except when very small tolerance of positioning is required, is normally not activated by masters during anchor deployment, possibly due to that the vessel being in constant motion and the continued communication between different parties. The masters are normally controlling the vessel manually or keeping the auto head condition. However, every master has his own experience and consequently different control strategy. As a result, it will be difficult to propose a general model to simulate the actions of the masters. The aim of the thrust utilisation plot in this paper, is to propose a reasonable measurement to estimate the capacity of the AHV in the planning stage, but not to look into details of a specific control strategy of a specific master.

In general, the typical AHV forward speed during anchor deployment is about 2–5 knots. Such a speed is considered to be quite low. In an unfavourable weather condition, when maintaining vessel position becomes the main task, the speed could be even lower. Moreover, as mentioned, the master will try to keep the AHV heading in line with the mooring orientation to avoid large angle of attack in a normal operation. Based on these two facts, the forward speed effect is therefore neglected and the angle of attack is assumed to be zero.

The flow chart of the proposed method is presented in Fig. 4. First, based on the given environmental conditions, which are normally given by sea-keeping analysis of the AHV, the mean environmental loads on the AHV can be estimated. Current-induced mooring loads, which can be influenced by current profiles and mooring line configuration, should also be considered. Then the resultant static external force on the vessel in the horizontal plane (surge, sway and yaw) can be obtained. The resultant lateral forces in sway and the resultant yaw moment are supposed to be balanced by the side tunnel thrusters and azimuth thrusters. The resultant longitudinal force in surge is supposed to be withstood by the main propellers. A thrust allocation method should then be applied to obtain the required thrust of the tunnel thrusters and azimuth thrusters, based on the lateral force and yaw moment. Comparing the required thrust with the available thrust, the tunnel and azimuth thrust utilisation plot can be established. The propeller thrust utilisation plot can be generated in a similar manner, except that the available bollard pull will be affected by side thrust usage and needs to be adjusted. Finally, the total thrust utilisation plot can be obtained by combining both the tunnel and azimuth thrust utilisation plot and the propeller thrust utilisation plot.

The main aim of this paper is to:

- Develop a numerical model suitable to simulate the anchor handling scenario in static analysis

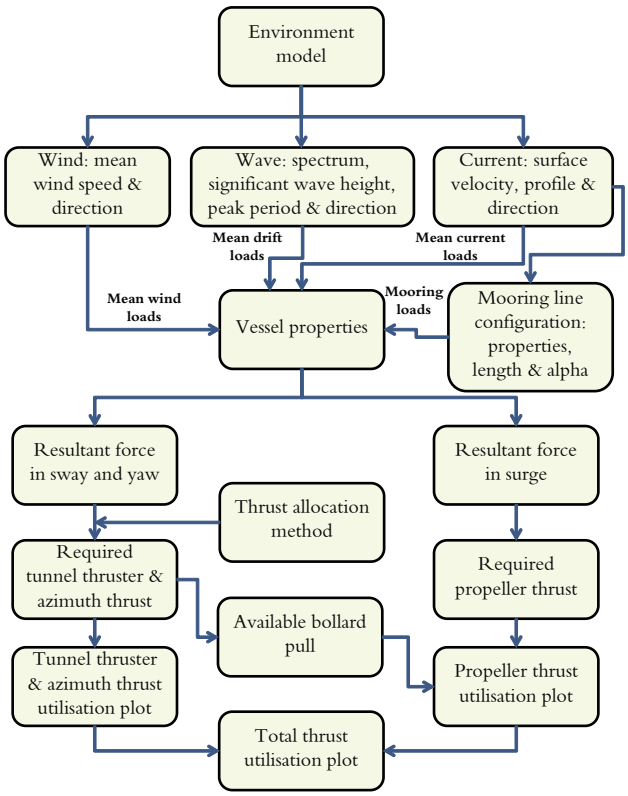

Fig. 4 Flow chart of the proposed method

- Estimate forces acting on the vessel and establish the thrust utilisation plot
- Apply the proposed method to the Bourbon Dolphin accident as a case study.

3 Theory background

Thrust utilisation plots represent the analysis of the equilibrium of the steady-state forces and moments of an AHV during anchor deployment in this study. The main concern is to estimate the external loads acting on the AHV correctly. The forces and moments in the horizontal plane are of interest. Components that have a high influence on the static external loads on the AHV are mean wave drift load, mean wind drift load, current load on the vessel and mooring load (see Fig. 4). Among these loads, the current load on the mooring line are not studied in previous limited open publications on an AHV. Augusto and Andrade [12] proposed a planning methodology for deep-water anchor deployment aimed at operational resource optimisation. Wennersberg [13] developed and implemented an anchor handling simulator based on the MSS toolbox [14]. The mooring line model in both studies was based on the catenary equation, which did not take the current forces acting on the mooring line into account. In practice, the current effect on the mooring line is usually not accounted for in a rig move procedure. Gunnu et al. [15] analysed the behaviour of an AHV in the horizontal plane in a uniform current field. The drifting behaviour of the vessel under different control forces (failure modes) was illustrated. However, the current loads on the mooring line were not studied explicitly. Moreover, wind and wave effects were not included. In this paper, a detailed model including wind, wave and current loads on both vessel and mooring line was established. In this way, more realistic external forces acting on the vessel can be estimated.

The SIMO [16] and the Riflex [17] are used as tools to perform steady-state analysis. Environmental loads on the vessel are obtained through SIMO, while mooring line loads are calculated from Riflex and added as external loads to the vessel. In the following section, the theory background applied will be addressed. The adopted thrust allocation method will be addressed as well.

3.1 Coordination system

The plain view of the coordinate systems applied is illustrated in Fig. 5. Two coordinate systems are used. Vessel position, mooring line configuration and environmental load direction are defined in the global coordinate system, (X_G, Y_G, Z_G). The global coordinate system is earth-fixed and the origin is defined at the rig end of the mooring line on the water plane. The vessel has its own local coordinate system, (x_B, y_B, z_B), which is at the projection of the centre of gravity on the water plane. The loads on the AHV are referred to the local coordinate system. The mooring line orientation is in line with the AHV heading because zero angle of attack is assumed in a normal operation.The direction definitions of wind (φ), wave (ψ) and current (γ) are also shown in Fig. 5. A value of 0° means that the weather is coming along the mooring line orientation, from stern to bow of the AHV, while a value of 90° indicates that the weather is coming perpendicularly to the mooring line orientation, from starboard to port of the AHV. The rig is not numerically modelled so that it is illustrated with dashed lines.

3.2 Wave drift loads

Mean drift loads are of importance in certain contexts, for instance, in the design of mooring system. Although the mean drift loads are relatively small in magnitude compared with the first order components, the mean drift loads may still contribute significantly to the total static environmental loads on the AHV. Therefore, it is important to obtain reasonable wave drift loads in this study.

When estimating the mean drift loads on an offshore structure, the common practice is to solve the first-order problem in potential flow theory. The mean drift loads can then be obtained by applying the theory of conservation of momentum (the far-field theory). More details can be found in [18]. A benchmark study on the calculation of potential theory among seven leading commercial codes was carried out by Naciri and Sergent in 2009 [19]. It is shown that all the codes involved predict very consistent first order quantities, as well as the mean drift coefficients calculated by the conservation of momentum theory. The WADAM code [20], one of the tested codes in the benchmark study, was used to obtain the mean wave drift coefficients for the Bourbon Dolphin vessel in this paper.

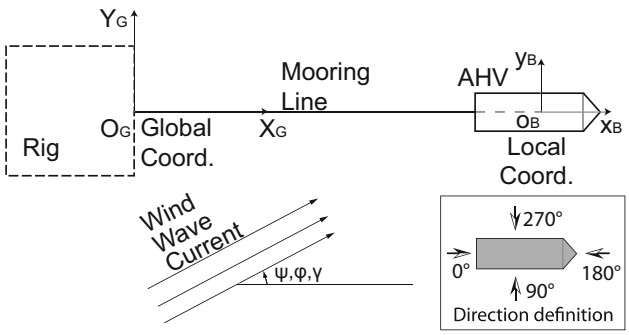

Fig. 5 Coordinate systems for an anchor handling operation and definition of direction

Table 1 Principal particulars of the Bourbon Dolphin

Properties	Notations	Values	Units
Length overall	L_{oa}	75.20	m
Length between perpendiculars	L_{pp}	64.91	m
Breadth	B	17.00	m
Depth	D_p	8.00	m
Draught at midships	D_m	5.80	m
Transverse projected area	A_t	314.34	m^2
Lateral projected area	A_l	653.28	m^2
Displacement	Δ	4,500	Tonne

The centre of gravity is located 6.90 m from keel and 32.03 m from aft perpendicular

The main particulars of the Bourbon Dolphin AHV are listed in Table 1. The 5.80 m draft is the draft when the Bourbon Dolphin accident happened. A convergence test on the meshing density of the panel model has been carried out. Good convergences of the required coefficients are observed when the element length is smaller than 0.6 m. In this paper, the results are based on a panel model with an element length of 0.5 m (see Fig. 6). The mean wave drift coefficients of the Bourbon Dolphin vessel in surge, sway and yaw are illustrated in Fig. 7a–c, respectively. These coefficients are imported into SIMO. The mean wave drift force can then be estimated for a given wave spectrum.

3.3 Wind drag force

The wind drag force is calculated based on the mean wind velocity on the vessel as follows:

$$F_{wx} = \frac{1}{2}\rho_a C_{wx}(\varphi) V^2 A_t \tag{1}$$

$$F_{wy} = \frac{1}{2}\rho_a C_{wy}(\varphi) V^2 A_l \tag{2}$$

$$M_{wn} = \frac{1}{2}\rho_a C_{wn}(\varphi) V^2 A_l L_{oa}, \tag{3}$$

where F_{wx}, F_{wy} and M_{wn} are the wind force in surge, in sway and wind moment in yaw, respectively; ρ_a is the density of air; C_{wx}, C_{wy} and C_{wn} are the wind drag coefficient in surge, sway and yaw, respectively; φ is the wind direction relative to the vessel heading (see Fig. 5); V is the wind velocity; A_t and A_l are the transverse and lateral projected area of the vessel superstructure, respectively; and L_{oa} is the length overall.

Information about the wind drag coefficient for specific vessels is quite limited in the public literature. To obtain the best approximation of the Bourbon Dolphin in the study, data of similar vessels were used. The wind drag coefficients were obtained in [21] for an offshore supply vessel (see Fig. 8).

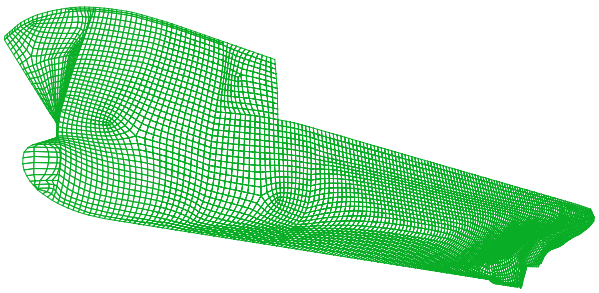

Fig. 6 Panel model of the Bourbon Dolphin, the port half

3.4 Current loads

The static current drag forces and moments are estimated using the following equations:

$$F_{cx} = \frac{1}{2}\rho C_{cx}(\gamma) U^2 B D_m \tag{4}$$

$$F_{cy} = \frac{1}{2}\rho C_{cy}(\gamma) U^2 L_{pp} D_m \tag{5}$$

$$M_{cn} = \frac{1}{2}\rho C_{cn}(\gamma) U^2 L_{pp}^2 D_m, \tag{6}$$

where F_{cx}, F_{cy} and M_{cn} are the current force in surge, in sway and current moment in yaw, respectively; ρ is the density of water; C_{cx}, C_{cy} and C_{cn} are the current drag coefficient in surge, sway and yaw, respectively; γ is the current direction relative to the vessel heading (see Fig. 5); U is the current velocity; B is the beam at midships; D_m is the draught at midships; and L_{pp} is the length between perpendiculars.

The current drag coefficients could be obtained both from model testing and from CFD calculation. In this paper, the current drag coefficients are obtained in the ShipX station keeping plug-in [22] (see Fig. 9). These coefficients were gathered from the MARINTEK model test for an offshore supply vessel similar to the Bourbon Dolphin.

3.5 Morison's equation

The modified Morison's equation was used to calculate current loads on the mooring line through the Riflex code. The drag force acting normal to the mooring line section with a length of dx is shown in Eq. 7:

$$\begin{aligned} dF_n = {} & \rho \frac{\pi D_h{}^2}{4} dx\dot{w} + \rho C_a \frac{\pi D_h{}^2}{4} dx(\dot{w} - \dot{s}) \\ & + \frac{1}{2}\rho C_D D_h dx(w - s)|w - s| \end{aligned} \tag{7}$$

where dF_n is the hydrodynamic force on an element with length of dx; ρ is the water density; D_h is the hydrodynamic diameter; w is the water particle velocity; C_a is the added

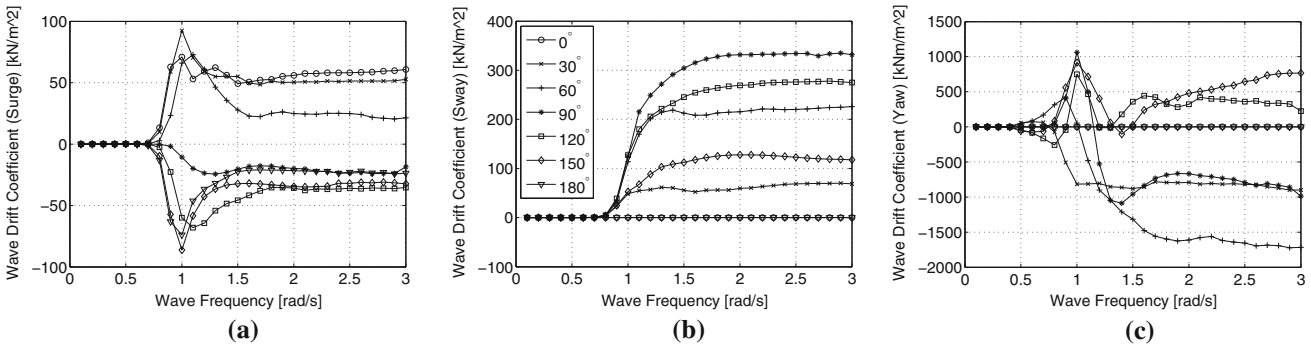

Fig. 7 Wave drift coefficients of the Bourbon Dolphin. **a** Surge, **b** sway and **c** yaw

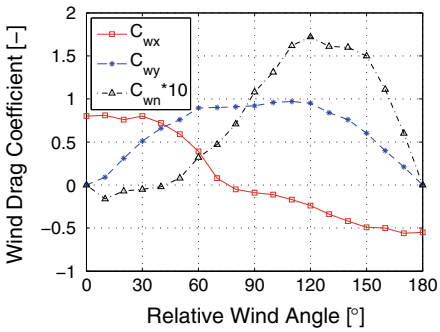

Fig. 8 Wind drag coefficients

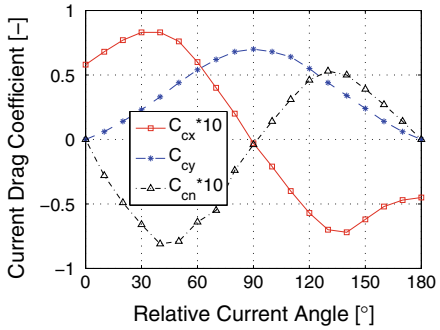

Fig. 9 Current drag coefficients

mass coefficient; s is the element velocity normal to cross section; and C_D is the quadratic normal drag coefficient. The first and second terms on the right represent the Froude–Krylov force and hydrodynamic mass force, respectively. The third term is the drag force. In a static calculation, the first two terms are zero, and only the drag force term remains.

3.6 Thrust allocation and thrust utilisation plot

The basic idea of the thrust utilisation plot, is to assess how much thrust capacity of the AHV is consumed to keep the vessel in a desired position and heading for a given weather condition. Therefore, the required thrust should be estimated first. The static external forces acting on the vessel, including mean wave drift load, mean wind load, mean current loads and mooring load can be determined by the theory mentioned above. Then, a thrust allocation method can be applied to obtain the demanded thrust for each position unit. The allocation method is usually formulated into an optimisation problem so that minimised power consumption can be achieved. In this study, the thrust allocation method follows the approach of Zhou et al. [23].

The general relationship between the control demand and the individual actuator demand thrusts is given by Eq. 8:

$$\boldsymbol{\tau}_{\mathbf{c}} = \boldsymbol{T}_{\mathbf{a}} \boldsymbol{T}_{\mathbf{th}}, \tag{8}$$

where $\boldsymbol{\tau}_{\mathbf{c}}$ is the vector of thrust and moment demand from the controller, $\boldsymbol{T}_{\mathbf{th}}$ is a vector of thruster demands in Cartesian coordinates, and $\boldsymbol{T}_{\mathbf{a}}$ is the thruster allocation matrix, defined as follows:

$$\boldsymbol{T}_{\mathbf{th}} = [T_{1x}\ T_{1y}\ \cdots\ T_{nx}\ T_{ny}] \tag{9}$$

and

$$\boldsymbol{T}_{\mathbf{a}} = [\boldsymbol{t}_1\ \cdots\ \boldsymbol{t}_n], \tag{10}$$

where n is the number of thrusters. In our case, only horizontal plane motions, i.e. surge, sway and yaw are to be balanced, the matrices $\boldsymbol{t}_i$ in Eq. 10 are given by Eq. 11:

$$\boldsymbol{t}_i = \underbrace{\begin{bmatrix} 1 & 0 \\ 0 & 1 \\ -l_{iy} & l_{ix} \end{bmatrix}}_{\text{azimuth thruster}}, \quad \boldsymbol{t}_i = \underbrace{\begin{bmatrix} 1 & 0 \\ 0 & 0 \\ -l_{iy} & 0 \end{bmatrix}}_{\text{main propeller}}, \quad \boldsymbol{t}_i = \underbrace{\begin{bmatrix} 0 & 0 \\ 0 & 1 \\ 0 & l_{ix} \end{bmatrix}}_{\text{tunnel thruster}} \tag{11}$$

where l_{ix} and l_{iy} are the longitudinal and transverse positions of the ith thruster, respectively.

In general, there will be more variables describing the thruster settings than available equations to solve (see Eq. 8) so that $\boldsymbol{T}_{\mathbf{th}}$ is not unique. This problem is usually

formulated as an optimisation problem by introducing a power minimisation condition. According to Fossen [24], the least-norm solution of $\boldsymbol{T}_{\mathbf{th}}$ could be achieved by finding the Moore–Penrose generalised inverse of $\boldsymbol{T}_{\mathbf{a}}$. The solution can be expressed in the following form:

$$\boldsymbol{T}_{\mathbf{th}} = \boldsymbol{T}_{\mathbf{a}}^{\dagger}\boldsymbol{\tau}_{\mathbf{c}} \tag{12}$$

$$\boldsymbol{T}_{\mathbf{a}}^{\dagger} = \boldsymbol{W}^{-1}\boldsymbol{T}_{\mathbf{a}}^{T}(\boldsymbol{T}_{\mathbf{a}}\boldsymbol{W}^{-1}\boldsymbol{T}_{\mathbf{a}}^{T})^{-1} \tag{13}$$

and

$$\boldsymbol{W} = \begin{bmatrix} w_{1x} & & & & 0 \\ & w_{1y} & & & \\ & & \ddots & & \\ & & & w_{nx} & \\ 0 & & & & w_{ny} \end{bmatrix} \tag{14}$$

where $\boldsymbol{T}_{\mathbf{a}}^{\dagger}$ is the generalised inverse of $\boldsymbol{T}_{\mathbf{a}}$, $\boldsymbol{W}$ is the weighting matrix in which the element w_{ix} is the cost to use the ith thruster in the surge axis, and w_{iy} is the cost to use them in the sway axis. The higher the cost in a DP system, the less thrust will be assigned to that thruster.

When the required thrust, i.e. $\boldsymbol{T}_{\mathbf{th}}$, is obtained by Eq. 12, the ratio between the required thrust and the available thrust of each thrust unit can then be calculated. Here, the available thrust is based on the thrust setup. Thrust loss is beyond the scope of this study and therefore is not considered. The maximum consumption ratio among all thrust units is used to represent the thrust utilisation for a specific weather direction. The results are usually presented in a rosette format, which shows the ratio as a function of weather direction.

4 Case study

The Bourbon Dolphin accident has been selected as the basic case for application of the suggested method. The static loads on the vessel during the accident are first investigated and discussed, including the mooring line loads in different current profiles. Then, a comparison between normal condition and accident condition (definition will be given in Sect. 4.1.2) is presented. Finally, the results of several sensitivity studies are shown. Some simplifications are made so that more general information can be obtained.

A short reminder of the Bourbon Dolphin accident [2]: the accident happened on the Rosebank oilfield in the western part of Shetland where the water depth was 1,100 m. The distance between the rig and the mooring position was approximately 3,000 m. The mooring line was approximately 3,500 m, of which 900 m was 84 mm chain and 920 m was 76 mm chain, plus 1,725 m of 96 mm wire. During the lowering of anchor, approximately 1,220 m of 83 mm wire was used by the Bourbon Dolphin. The Bourbon Dolphin ran out all the chain (approximately 1,820 m) for the last anchor (no. 2). Then the vessel drifted considerably off the mooring line and asked the rig for assistance. However, the attempt at chain grappling by another vessel failed. At that moment, the vertical angle α (the angle between the mooring line and the vertical plane, see Fig. 3) was 38°. Then the vessel capsized during a turn. See Fig. 1 for the track plot of the Bourbon Dolphin before the accident happened.

4.1 Load analysis

In this section, the external forces on the AHV during operation are analysed. First, the current loads on a free-spanning mooring line are investigated. Then, the total forces acting on the vessel under different environmental conditions are presented.

4.1.1 Mooring line loads

While mooring line analysis is commonly conducted for moored floating structures, study of the effect of a mooring line during an AHO is not common. As the water depth increases, the weight of the mooring line increases, which demands a higher capacity for the AHV. A higher winch capacity on board is needed due to the mooring line weight. Meanwhile, the drag force induced by the current increases as the length of the mooring line increases. The current-induced mooring load will consume a part of the lateral thrust forces, which is usually neglected in shallow waters. Although the shape and tension of a mooring line in calm water can be predicted well by the traditional catenary equation, the situation becomes complicated if the current load is applied. For instance, the shape of the mooring line will depend on the weight and buoyancy as well as the current field and thus the loads applied on the vessel could vary. Therefore, the effect on the loads coming from the mooring line is of interest.

This subsection describes a parametric study to assess the effect of current on the mooring line. A two-end-fixed free-spanning mooring line with uniform cross-section is placed into different current profiles. A sketch of this study is illustrated in Fig. 10. The mooring line is assumed to be aligned with the AHV centre line. The aim is to analyse the force on the AHV end. The parameters involved are shown as follows: length of mooring line L, vertical angle α, types of mooring line, diameter of mooring D, surface current velocity U, current direction γ and current profile. With a different end distance and a different vertical angle, the mooring line will have different initial shape (in still water). Then the current force is applied (with varied

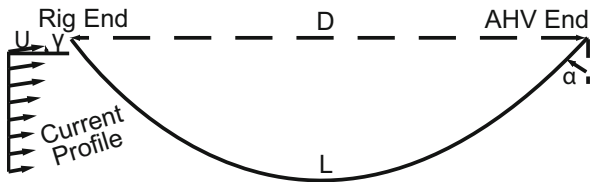

Fig. 10 Sketch of two-end-fixed mooring line in current

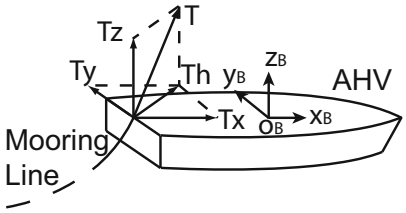

Fig. 11 Force components of mooring line tension

direction and velocity) and the mooring line will have a modified shape based on the current condition. As a result, the distribution of tension along the mooring line will be changed as well. Iterations should be performed to obtain the final static shape of the mooring line. Once the static shape is found, the tension along the mooring line is also determined. Finally, the force components acting on the vessel can be obtained.

The significant force components in the total tension T are the longitudinal force component T_x and the lateral force component T_y (see Fig. 11). The total tension T is related to the capacity of the main winch on board. The winch capacity should be greater than the total tension coming from the mooring line, or the winch might be unable to handle the mooring line. The longitudinal force component T_x is directly linked to the bollard pull. If the bollard pull of the vessel is smaller than this component, the vessel will be pulled backward by the mooring line. The lateral component, T_y, could consume part or even all of the lateral positioning capability of the vessel. If the amount is large, T_y could hamper the vessel bollard pull as well. In practice, T and T_x are quite high compared with the current loads and not affected much . Emphasis is placed on the current effect on T_y.

The selected length of the mooring line in this study is 1,800 m, which is almost the same as what Bourbon Dolphin had paid out (1,817 m) before the accident happened. Based on the rig move plan that was carried out during the Bourbon Dolphin accident, two types of mooring line were used, including the stud chain and the wire with wire core. Within each type of mooring line, two diameters were selected to study the effect of diameter. So in total, there were four mooring lines that were studied, and the properties of these mooring lines are summarised in Table 2. In fact, the type of mooring line used is normally selected according to the mooring performance analysis of the mooring system rather than the AHO analysis. The comparison between these mooring lines, however, can show the influence of mooring line properties on the force components within the same practical project.

In the actual practice, the vertical angle between the mooring line and the vertical axis (α) is usually between 20° and 60°. This angle describes the relative importance of the horizontal and the vertical components of the total tension. A different angle α can be achieved by altering the distance (D) between the two ends of a mooring line. For the purposes of convenience, the same distance is applied on all four types of mooring line for a nominal α value. Due to the difference in axial stiffness between chains and wires, there are small differences in the actual angle α of

Table 2 Mooring line properties

Properties	Units	Mooring line type			
		Stud chain		Wire	
Geometry					
Diameter (nominal diameter)	m	0.084	0.076	0.096	0.083
Equivalent diameter	m	0.159	0.144	0.077	0.066
Weight and buoyancy					
Mass per unit length	kg/m	154.50	126.50	37.77	27.49
Weight per unit length	kN/m	1.516	1.241	0.361	0.270
Buoyancy per unit length	kN/m	0.199	0.164	0.047	0.035
Weight per unit length in water	kN/m	1.317	1.077	0.314	0.235
Structure					
Axial stiffness	kN	7.13×10^5	5.83×10^5	3.72×10^5	2.78×10^5
Hydrodynamics					
Normal drag coefficient	–	2.6	2.6	1.2	1.2
Tangential drag coefficient	–	1.4	1.4	0.0	0.0

The nominal diameter of chains represents the bar diameter. The equivalent diameter is for a line with constant volume along its length. The drag coefficient is defined on the nominal diameter. The drag coefficients are obtained from DNV recommended practice [28]

Table 3 Relationship between D and α for a 1,800-m-long mooring line

D (m)	Actual α(°)		Nominal α (°)
	Stud chain	Wire	
773	10.00	10.01	10
1,137	19.95	19.99	20
1,370	29.99	30.05	30
1,501	37.95	38.06	38
1,589	44.96	45.12	45
1,716	59.73	60.18	60
1,787	74.09	75.92	75

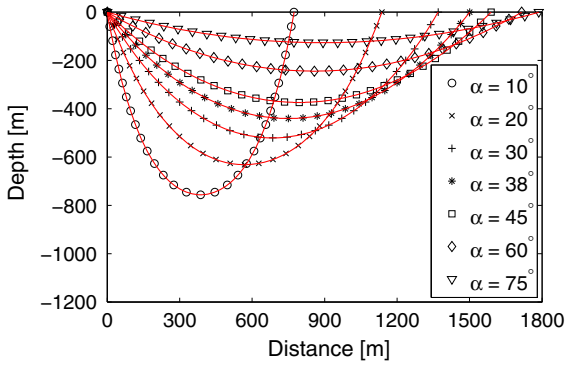

Fig. 12 Static shape of a 84-mm K4 studded chain mooring line for different angle α, $L = 1,800$ m. Analytical solutions are presented with *red solid lines*. Riflex results are presented with *different markers* (colour figure online)

the mooring lines. However, the difference between the actual and nominal value is small. The selected distance and the corresponding α (both actual and nominal) are tabulated in Table 3. The nominal α varies from 10° to 75°. Hereafter, angle α in this paper refers to the nominal value. The static shapes of 1,800-m-long mooring line with 84 mm chain properties (with different α) in still water, calculated by Riflex, are illustrated in Fig. 12 with markers. The analytical solutions of the elastic cable line equations, see [18], are also presented in Fig. 12 (as red solid lines). As shown, the Riflex results are in very good agreement with the analytical solution.

The current profile, velocity and direction have an influence on the mooring line shape, thus they have an effect on the force components as well. Six current profiles in total have been chosen to evaluate the effect. The six current profiles are uniform, linear sheared, uniform with 50-m slab, linear sheared with 50 m, Ormen Lange field (representing the profile in the North Sea) and Loop eddies current field (representing the profile in the Gulf of Mexico). The first two profiles are theoretical current profiles for deep water. The middle two profiles are the design profiles proposed by DNV recommended practice [25] for

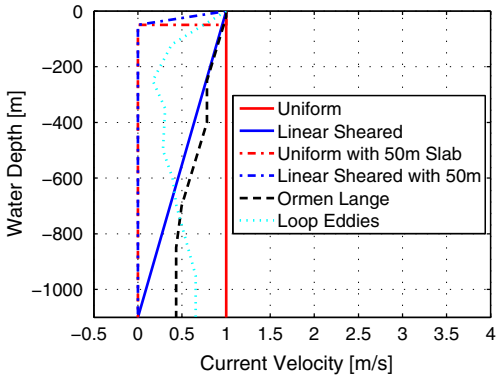

Fig. 13 Current profiles

wind generated current, in which the current velocity is zero below 50 m. More detail about the last two current profiles can be found in Rustad et al. [26]. According to ISO 19901-1 [27], the indicative value for 1-year-return surface current speed in the west of Shetland is 1.64 m/s. This value coincides with the maximum estimation of current speed (3 knots) during the accident in terms of order. The normalised current velocity profile, with a surface velocity equals to 1 m/s, are illustrated in Fig. 13.

The influence of the current profiles as well as the angle α on the lateral force component T_y is shown in Fig. 14. The length of the mooring line is 1,800 m and the current direction is normal to the mooring direction($\gamma = 90°$) with a surface velocity of 1.0 m/s. In this case, T_y represents half of the total lateral current loads on the mooring line. In general, the difference between stud chain and wire are quite significant. The T_y of chains is more or less twice the magnitude of the T_y of wires in most cases. Therefore, deploying mooring line with chain sections is usually more demanding than using wire sections (of the same length) because the weight will be heavier and possible current drag loads will be higher. The diameters have less importance for the current loads within the same type of mooring line. The maximum difference due to diameter occurs in the uniform current field in stud chains. However, the difference is less than 10 kN (1 tonne).

The T_y has a strong angle α dependence in all profiles except the uniform profile mainly because a different angle α means a different spanning depth of the mooring line. In a uniform current field (see Fig. 14a), T_y is almost the same among all angles α for the same property. This equality is easy to understand because the profile is uniform and therefore the mooring lines are subjected to almost the same current loads. A 1,800-m 84 mm mooring chain can lead to approximately 100 kN (10 tonnes) in T_y in 1 m/s uniform current. In a linear sheared current profile (see Fig. 14b), T_y increases from 40 kN to almost 90 kN as the angle α varies from 10° to 75°. Within the practical range

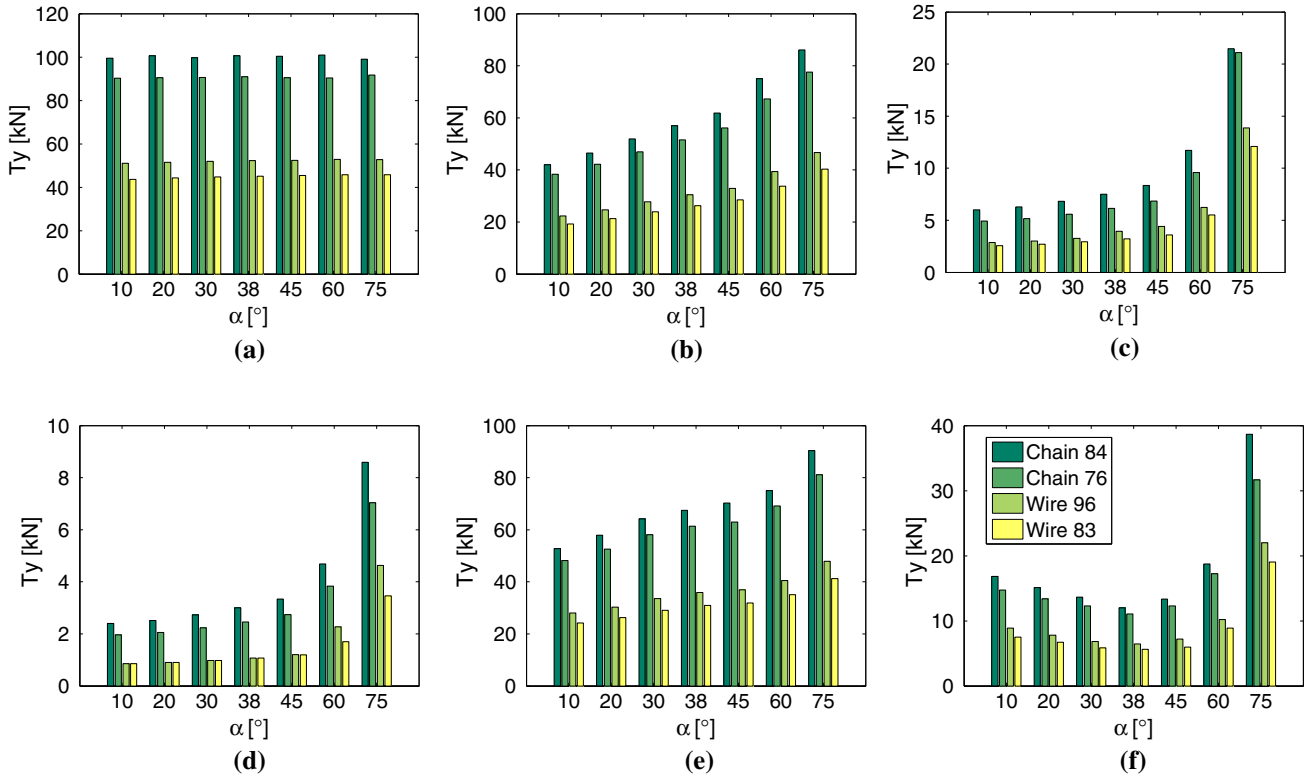

Fig. 14 Lateral force component (T_y, see Fig. 11) comparisons for different current profiles and different angle α (see Fig. 10), $\gamma = 90°$, $U = 1.0$ m/s, $L = 1,800$ m. **a** Uniform current profile, **b** linear sheared current profile, **c** slab uniform current profile (50 m depth), **d** linear sheared current profile (50 m depth), **e** Ormen Lange field current profile and **f** loop eddies current profile

of α, for example, 38°, the current-induced lateral force is more than 55 kN.

In the two design profiles of wind generated current, T_y are smaller compared with other cases because current only affects the very upper part of the mooring line (within 50 m water depth). Figure 14c shows that there is a jump in the magnitude for all mooring lines when α is 75° because the spanning depth of the mooring lines is small in this case (see Fig. 12) and a much greater portion of the lines is exposed to the slab current. Therefore, the total current loads on the lines are much higher. In the linear sheared profile with 50 m depth, the phenomenon is similar (see Fig. 14d). Within the practical range of α, however, T_y is very small for wind generated current profiles.

In regard to the actual current profile, the results are more interesting. In the current profile at the Ormen Lange field, the current remains quite strong over the water depth resulting in a relatively high drag load on the mooring line (see Fig. 14e). In the Norwegian sector, AHV might have a higher demand on the thrust capacity due to possibly higher current load on the mooring line. In the current profile at the Gulf of Mexico (GOM), the minimum T_y occurs when the angle α is equal to 38° (see Fig. 14f), due to the uniqueness of this current profile. There is a drop of the current strength in approximately 350 m of water depth. However, the current gradually becomes stronger as the water depth increases. To keep the main part of the mooring line in the low current strength region might be an advantage to take in the GOM.

The uniform current profile is used to investigate the effect of current direction and velocity on T_y. The current velocity varies from 0.5 to 2.0 m/s. A value of 2.0 m/s is too high for an operation weather window and is just for illustration. However, 1.0 m/s is usually chosen as the design criterion (the same as the Bourbon Dolphin rig move procedure), therefore the value is quite reasonable. Because the α has no influence on T_y in a uniform current field, there is no need to vary α. The T_y induced current on an 1,800-m 84 mm mooring chain with angle α equal to 38° is presented in Fig. 15. The figure shows that T_y is generally proportional to velocity squared. In the 1.5 m/s current speed, current load on an 1,800-m 84 mm stud chain can be more than 220 kN, which is approximately 22 tonnes. If this happened in the real world, the AHV would be in a very challenging situation to maintain position. The maximum values occur at 90° in a low current speed profile and shift to 80° when in a high current speed profile.

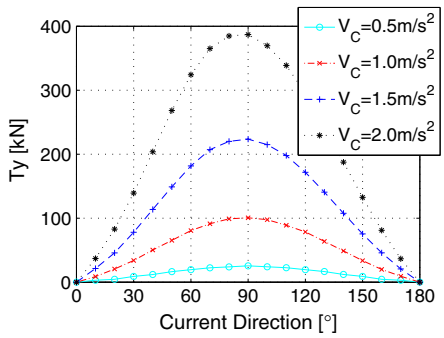

Fig. 15 Lateral force component (T_y) comparisons for different current directions and velocities, uniform current profile, $L = 1,800$ m, $\beta = 38°$, 84 mm chain

Due to the considerable differences in lateral mooring loads among different current profiles, it is very important to take the mooring line effect into account and apply the current profile in practice as closely as possible. Further discussion will be provided in the following subsections.

4.1.2 External loads on the vessel

The external forces acting on an AHV depend on the vessel dimensions and environmental conditions as well as the mooring line configuration. The main particulars of the Bourbon Dolphin anchor handling vessel are listed in Table 1. The 5.80 m draft is the draft when the Bourbon Dolphin accident happened.

According to the accident report [2], the weather conditions referred to in the rig move procedure mooring analysis for the Bourbon Dolphin are listed as follows:

- Maximum waves of 4.0 m, significant wave height (H_s) is approximately 2.2 m, with a wave period (T_p) of 8.5 s
- Wind speed (V_W) 10 m/s (19.4 knots)
- Current speed (V_C) 1.0 m/s (1.94 knots).

The weather conditions during the day of the accident were different from the rig move procedure. Based on several assessments from weather forecasts and testimony of masters, the weather observations were relatively consistent on wave and wind, while there were strong disagreements on the current. The actual weather situation is listed as follows:

- Significant wave height was approximately 3.5 m (max wave approximately 7 m) with a wave period of 7–8 s.
- Mean wind strength was approximately 18 m/s (30–35 knots).
- Estimated current speed varied from 0.3 to 1.5 m/s (0.6–3 knots).

Table 4 Environmental conditions

		Normal	Accident	Units
Wave	H_s	2.2	3.5	m
	T_p	8.5	7.0	s
Wind	V_W	10	18	m/s
Current	V_C	1.0	1.0	m/s

Based on the above information, two environmental conditions are defined in this study. The condition used in the rig move procedure is denoted as the "Normal" condition, while the actual weather condition is denoted as the "Accident" condition. The details of these two weather conditions are tabulated in Table 4. The selected wave spectrum is the Jonswap spectrum and the wind field is considered as constant with uniform profile. The current profile used here is the Ormen Lange profile, which is supposed to be the most suitable one among the six studied profiles. Due to the inconsistency on the surface current speed estimation in the accident condition, the current speed in the accident condition is set the same as the current speed in the rig move procedure, i.e. 1 m/s. In this way, the influence from deterioration of the wind and the waves can be investigated.

Static analyses were performed to obtained static loads on the Bourbon Dolphin under these two sets of conditions. No weather misalignment was considered. The mooring line was attached at the stern of the AHV at the centre line. The distance between the attach point to the centre of gravity is 37.23 m. The mooring line was set as 1,800 m of 84 mm chain with the angle α equal to 38°. The configuration is similar to that in the accident. The lateral force and yaw moment with respect to the centre of gravity of the Bourbon Dolphin as a function of weather direction is shown in Fig. 16. The current load acting on the vessel is denoted as "current", while the mooring load acting on the vessel due to current is denoted as "mooring". Because the current conditions are the same in both normal and accident conditions, the "current" and "mooring" loads in both case remain the same.

For lateral force components, the highest total force occurs around the beam sea condition, i.e. 90°. The maximum total force in the accident condition is approximately 67 % higher than that in the normal condition. In the normal condition, the current load on the vessel is predominant, while the other three are quite similar in magnitude. In the accident condition, the wave drift force becomes stronger and contributes the most to the total load. The mean wind load also increases significantly.

For the yaw moment components, the trend is not as clear as the lateral force because the peak value of each component does not occur in the same weather direction. In general, high total yaw moment appears at a stern

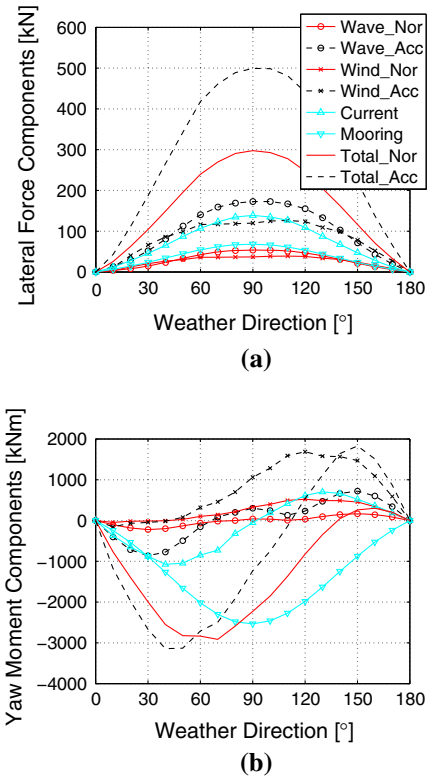

Fig. 16 Force components for a variable weather direction, " Nor" and " Acc" indicate normal and accident conditions, respectively. **a** Lateral force components and **b** yaw moment component

quartering sea under normal conditions. Because the wave drift moment increases significantly in the accident condition, especially in a bow quartering sea, high yaw moment occurs at both stern and bow quartering sea in the accident condition.

As the total external yaw moment does not reach the maximum value as the lateral force does in beam sea conditions, the most severe case might not occur in beam sea conditions. This situation will be illustrated in the following subsection.

4.2 Vessel positioning capability

The propulsion and thrust setup for the Bourbon Dolphin are sketched in Fig. 17. The vessel has one bow tunnel thruster

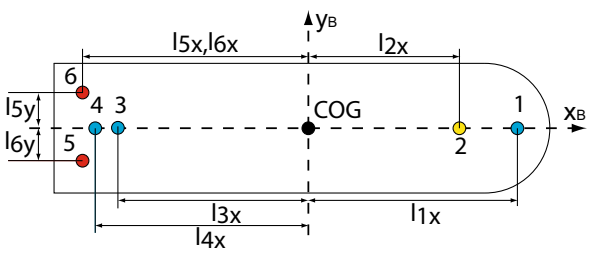

Fig. 17 The thruster arrangement schematic of the Bourbon Dolphin

Table 5 Propulsion and thrust setup for the Bourbon Dolphin

Propulsion unit	Thrust no.	Power (kW)	Force (kN)	l_{ix} (m)	l_{iy} (m)
Bow tunnel thruster	#1	883	149	27.37	0.00
Bow azimuth	#2	883	158	19.80	0.00
Stern tunnel thruster 1	#3	590	100	−24.83	0.00
Stern tunnel thruster 2	#4	590	100	−27.93	0.00
Main propeller 1	#5	6,000	967	−29.60	−4.65
Main propeller 2	#6	6,000	967	−29.60	4.65

(#1), one bow azimuth thruster (#2), two stern tunnel thrusters (#3 and #4) and two main propellers (#5 and #6). The numbering and position information for these units is listed in Table 5. The main propellers are normally used to provide bollard pull for the AHV to balance the mooring weight and water resistance. The tunnel thrusters are normally used to withdraw later loads and external yaw moment. The azimuth thruster can produce force in different directions depending on need. The capability of the vessel to withstand drift and maintain heading is of primary concern in this study. The tunnel thrusters and azimuth are assumed to be used to balance all the lateral forces and yaw moments. The two main propellers provide only longitudinal forces. Therefore, the thrust allocation scheme only involve the three tunnel thrusters and the bow azimuth thruster. The cost for these thrusters is assumed to be the same and set as 1 in Eq. 14. The lateral thrust utilisation plot is first applied to the Bourbon Dolphin accident. Then the propeller thrust utilisation and total thrust utilisation plots will be looked into.

Due to symmetries of the vessel about the longitudinal axis, in this study the thrust utilisation plots are also symmetrical about the same axis. In the case of other vessels, the plots could be asymmetric.

4.2.1 *Bourbon Dolphin accident*

First of all, the proposed lateral thrust utilisation plot is applied in the Bourbon Dolphin accident, in both normal and accident conditions (see Table 4). The current profile here is from Ormen Lange. The mooring line configuration also remains the same as a 1,800 m 84 mm mooring chain, with α as 38°. The result is illustrated in Fig. 18. The black solid line in the figure is used to highlight the 100 % circle, which is not supposed to be exceeded.

In general, the plots for both conditions show a similar trend. The thrust utilisation becomes low when the weather direction is toward 0° or 180°, because of low lateral force and moment. As the weather is coming more from the beam sea, the utilisation level increases significantly. However, the highest consumption occurs at approximately 70° and 290° instead of exactly at the beam sea condition. The figure shows clearly that the Bourbon Dolphin is

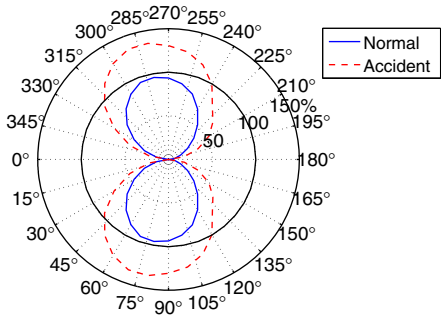

Fig. 18 Lateral thrust utilisation plot for normal conditions and accident conditions, $L = 1,800$ m, $\alpha = 38°$, Ormen Lange current profile

capable of handling the situation under normal conditions. Under the accident conditions, however, there is such a wide range of weather directions that the vessel is not capable of maintaining position. Moreover, according to the accident report, the prevailing weather direction in the accident event was from the southwest. Taking the mooring line 2 orientation (north by northwest) into account, a weather direction of approximately 290° is found in our coordinate system (see the actual direction from Fig. 1 and the definition of direction from Fig. 5). Figure 18 shows that at a direction of 290°, the thrust utilisation ratio almost reaches the maximum, which is approximately 135 %. The Bourbon Dolphin might have been in the most unfavourable weather situation during the accident condition when it began to drift, in terms of lateral positioning capability.

The variation of the required thrust force of the three tunnel thrusters and the azimuth are presented in Fig. 19. Only results from 0° to 180° weather directions are shown due to symmetries. The results are consistent with the force and yaw moment components plot (Fig. 16b). Other than balancing the lateral forces on the vessel, an unequal thrust distribution is required between the bow and stern to counteract the external yaw moment. When the yaw moment tends to make the bow of the vessel turn to the starboard side, i.e. a negative yaw moment exists, more thrust induced moment from the stern rather than the bow is demanded to maintain the heading of the vessel, resulting in a higher required thrust on the stern units than on the bow units (for example, in the 60° case in normal conditions). When a positive yaw moment acts on the vessel, more thrust is needed from the two bow units (for example, in the 150° case under accident conditions). As the available thrust of the stern tunnel thrusters is approximately 30 % lower than the available thrust of the bow units (see Table 5), the stern units are much easier to overload. In all cases of exceeding capacity under accident conditions, the stern thrusters (#3 and #4) have the highest usage.

The most critical weather directions under normal and accident conditions are 80° and 70°, respectively. The

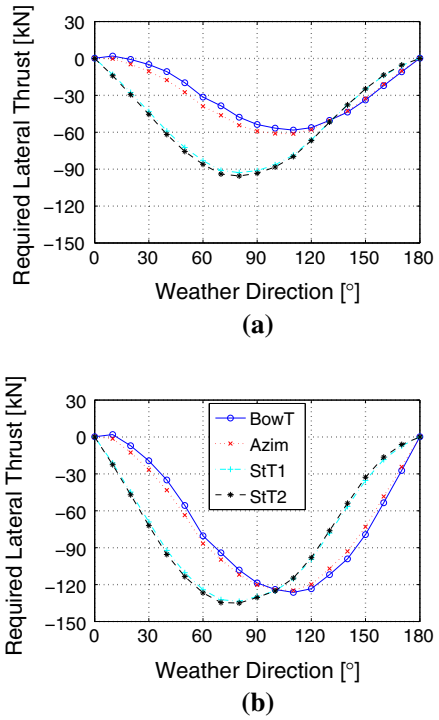

Fig. 19 Required lateral thrust force of different unit as a function of weather direction, " BowT", " Azim", " StT1" and " StT2" represent bow tunnel thruster (#1), azimuth thruster (#2), stern tunnel thruster 1 (#3) and stern tunnel thruster 2 (#4), respectively. **a** Normal conditions and **b** accident conditions

detailed force and moment components in these situations are tabulated in Tables 6 and 7. The current load acting on the vessel is denoted as "current", while the mooring load acting on the vessel is denoted as "mooring". At 80° under normal conditions, the total lateral force is 290.70 kN. Current load on the vessel contributes 46 % to the total loads. Together with the lateral loads from the mooring line due to the current, the total lateral loads induced by current is 69 %. For the yaw moment, contribution from mooring line is predominant. All these data emphasise the importance of the current effect in anchor handling operation.

Under accident conditions at 70°, the lateral force is as high as 461.30 kN, which will consume most of the lateral thrust that is available (507 kN). The lateral force together with the yaw moment lead to insufficient thrust. The wave drift force becomes the most important with a 35 % contribution in the lateral force as a single source. But the total lateral loads contribution induced by current (including the lateral mooring load) is 40 %. For the yaw moment, the mooring line loads contribute most as 92 % and current load on the vessel is 29 %. But wave drift and mean wind loads have a negative effect, which results in lower total yaw moment.

Forces in surge in both cases are dominated mainly by the mooring loads.

Table 6 Detailed load components under normal conditions, 80°

Item	Actual value			Percentage (%)		
	Surge (kN)	Sway (kN)	Yaw (kNm)	Surge (–)	Sway (–)	Yaw (–)
Wave drift	0.33	52.54	−2.17	0	18	0
Wind	−0.97	36.56	214.50	0	13	−8
Current	1.01	134.80	−318.90	0	46	12
Mooring	−933.90	66.74	−2,485.00	102	23	96
Total	−919.60	290.70	−2,591.00	100	100	100

Table 7 Detailed load components under accident conditions, 70°

Item	Actual value			Percentage (%)		
	Surge (kN)	Sway (kN)	Yaw (kNm)	Surge (–)	Sway (–)	Yaw (–)
Wave drift	−26.09	159.20	81.57	−3	35	−3
Wind	5.01	117.20	460.10	−1	25	−18
Current	2.01	122.90	−730.70	0	27	29
Mooring	−928.70	61.94	−2,306.00	105	13	92
Total	−881.60	461.30	−2,495.00	100	100	100

4.2.2 *Effect of current profile*

Based on the findings in the previous subsection, current loads are of significant importance in the AHO. The current profile has a high influence on the mooring load, which has already been shown. Therefore, a parametric study was carried out to investigate the influence on the lateral thrust utilisation plot from current profiles. All profiles shown in Fig. 13 were used. The mooring line configuration also remains the same as an 1,800 m 84 mm mooring chain, with α is 38°. Both normal and accident conditions were tested and the results are presented in Fig. 20.

Figure 20 shows that the results can be classified into three groups. Group one includes the two wind generated-current profiles and the loop eddies profile. Under both sets of conditions, the vessel can maintain sway and heading in these current profiles, except that there is a small exceeding for the loop eddies profile under accident conditions. Because the current load on the mooring line in these three profiles is quite low (see Fig. 14), the results can be considered as no current effect applied on the mooring line. The second group includes the uniform profile. The positioning capability of the vessel is not sufficient even under normal conditions for certain directions, let alone in accident conditions. The remaining profiles form the third group, including the linear sheared profile and the Ormen Lange profile. A vessel in this profile group is capable of withstanding the external lateral force under normal conditions but will drift-off under accident conditions at certain weather directions.

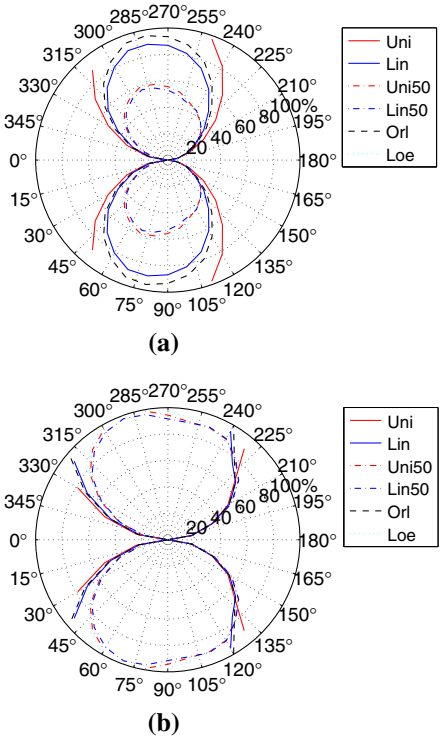

Fig. 20 Lateral thrust utilisation plot with different current profiles, $L = 1,800$ m, $\alpha = 38°$, "Uni", "Lin", "Uni50", "Lin50", "Orl" and "Loe" represent the six current profiles in the same order as shown in Fig. 13. **a** Normal condition and **b** accident condition

Clearly using the uniform current profile overestimates the current loads on the mooring line and thus leads to conservative results. Profiles in group one are reasonable, provided that the wind induced current are dominant in the region where the operation is taking place. The current profile effect in this group can be neglected because the lateral mooring load is small (see Fig. 14). The linear sheared profile and the Ormen Lange profile are the most suitable profiles to use in the Bourbon Dolphin case. Applying these profiles gives a much more realistic external forces description for the vessel. Therefore, more reliable thrust utilisation plots can be obtained.

4.2.3 *Effect of mooring line configuration*

During the deployment of the anchor, the mooring line is paying out based on the rig move procedure and the judgment of the tow master. As the length of mooring line in water increases, the loads acting on the vessel vary as well. If the angle α remains the same, the longer the mooring line is, the more loads the vessel needs to carry in the longitudinal direction. The current loads on the mooring line also vary, depending on the current profile (but it usually increases). As previously mentioned, the bollard pull was materially reduced due to the use of thrusters

during the Bourbon Dolphin accident. From the accident report, the total bollard pull of the Bourbon Dolphin reduced from 180 to 125 tonnes at maximum side thruster loading. How the propeller usage is influenced by the mooring line is of interest. Therefore, the propeller utilisation plot is introduced in the same way as the tunnel thrusters and azimuth, taking the reduction effect into account in a simple manner. Due to the lack of information, the two propellers are assumed to provide 180 tonnes of thrust forward in total when the lateral thrust usage is zero. As the lateral thrust utilisation increases, the thrust from the propellers decreases linearly to 125 tonnes when the lateral thrust utilisation reaches 100 %. In practice, the real reduction relationship can be applied.

First, the demanded thrust of the tunnel thruster and azimuth is estimated, summed and compared with the total available side thrust. Applying the ratio in the relationship of the propeller deduction, the "available" thrust of the propellers can then be obtained. Thus, the thrust utilisation plot for the propeller can then be generated. The maximum value between the thruster and propeller is used to establish the total thrust utilisation plot.

A parametric study has been carried out to examine the influence on the total thrust utilisation plot, with respect to different mooring line pay-out lengths. Different lengths of mooring line can represent different stages of the anchor handling process. Both normal and accident conditions were tested. The results are presented in Fig. 21. With a longer pay-out mooring line, the side thrust utilisation gradually increases when the weather is coming from the side, and remains low in a head sea and following sea conditions (see Fig. 21a, d). Under normal conditions, the vessel can handle the lateral external loads for all weather directions with a mooring line up to a length of 1,800 m. With longer pay-out length, the vessel is lack of position capability at approximately 80° and 280°. However, under accident conditions, the vessel is vulnerable in stern quartering sea weather conditions. Even with a 600 m length of mooring line the thrust usage is over 100 %.

The propeller utilisation is dominated mainly by the length of the mooring line (see Fig. 21b, e). As the length of the mooring line increases, increasing tension is applied on the AHV due to the increasing total weight of the line. The propeller utilisation increases quite evenly. However,

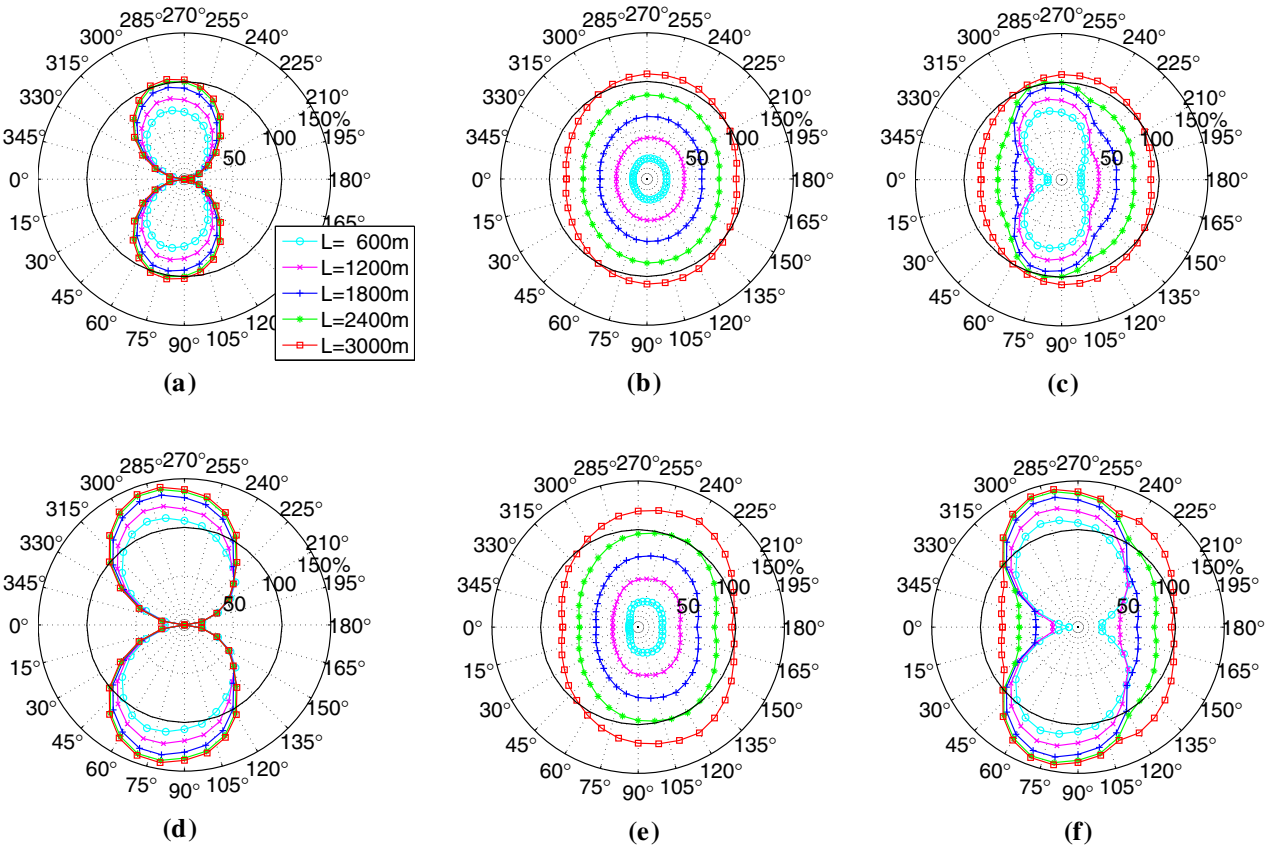

Fig. 21 Thrust utilisation plots with varying mooring line pay out length, $\alpha = 38°$, Ormen Lange current profile. **a** Thruster and azimuth, normal conditions, **b** propeller, normal conditions, **c** total, normal conditions, **d** thruster and azimuth, accident conditions, **e** propeller, accident conditions and **f** total, accident conditions

the propeller utilisation is also influenced by the side thrust usage because the available propeller thrust is lower in side weather conditions comparing to other weather directions. As a result, higher propeller utilisation is observed in about beam sea conditions, especially under accident conditions. The propeller utilisation is higher in head sea (180°) than in following sea condition (0°) because in head sea condition, the direction of current-induced loads on the mooring line is opposite to the thrust of the propellers, so the required bollard pull is higher, and vice versa.

The total thrust utilisation plots for normal and accident conditions are shown in Fig. 21c and f. Under normal conditions, the vessel can fulfil the task in all weather directions. However, if the length of mooring line reaches 3,000 m, the propellers will be overloaded in side weather conditions due to the increased mooring weight and bollard pull deduction. Under the accident conditions, the weather directions in which the vessel can maintain position are limited to a small spread around the following sea. As a result, if this information were provided before the operation commenced, the tragedy might have been averted.

5 Conclusion

Anchor handling operations, like all human activities, are potentially hazardous. The mooring line represents a significant risk factor for the anchor handling vessel due to its heavy weight as well as possible current loads, especially in deep water. Considerable drift is considered an initial event in the notable Bourbon Dolphin accident and should be prevented. Therefore, there is a need to establish a method to quantify the positioning capability for anchor handling vessel during anchor deployment.

In this paper, the thrust utilisation plot is proposed to present the positioning capability of the anchor handling vessel in a basic anchor deployment operation. Emphasis has been placed on obtaining realistic static loads on the vessel, including mean wind loads, mean wave drift load, mean current loads and mooring line loads.

A case study was carried out based on the Bourbon Dolphin case. The main conclusions can be summarised as follows:

- Lateral mooring loads vary significantly in different current profiles, therefore it is important to apply a reasonable current profile and take the mooring line effect into account.
- The thrust utilisation plot is useful to demonstrate the most critical weather direction. When the Bourbon Dolphin began to drift during the accident event, it might have been in the most unfavourable weather direction, which is 290°, in terms of lateral positioning capability.
- Current loads represent the most important loads in the Bourbon Dolphin case (with the Ormen Lange field current profile). Current loads on the vessel together with current-induced mooring loads contributed up to 69 % (in normal condition) and 40 % (in accident condition) to the total lateral loads.
- In regions where wind driven current is dominant, current loads on the mooring line can be neglected. In regions where a characteristic current profile exists, current-induced mooring line load should be considered in the thrust utilisation plot, for instance, in the Ormen Lange field in Norwegian waters.
- When the vessel deploys a very long mooring line, the limitation might come from the available propeller thrust due to heavy mooring weight and bollard pull deduction.

In general, the proposed method (see Fig. 4) is easy to implement and is useful for presenting the limitations of the anchor handling vessel before the operation commences. The proposed method is a good tool for defining vessel specific limitations, selecting a proper anchor handling vessel in terms of positioning capability during the planning stage and can also serve as the basis for establishing critical scenarios that are valuable for crew training in a simulator.

Acknowledgments This work was carried out at the Centre for Ships and Ocean Structures at the Faculty of Engineering Science and Technology, Norwegian University of Science and Technology (NTNU), Trondheim, Norway. The authors would like to acknowledge the financial support from the SINTEF Fisheries and Aquaculture granted through CeSOS. MARINTEK is acknowledged for providing software licenses for SIMO and Riflex. The authors would also like to thank Master Åge Muren from Farstad Shipping ASA for his support and helpful discussions on practical issues related to anchor handling.

References

1. Saasen A, Simpson M, Ribesen B, Høj J (2010) Anchor handling and rig move for short weather windows during exploration drilling. In: The IADC/SPE drilling conference and exhibition, New Orleans
2. Lyng I (2008) Official norwegian reports: the loss of the "bourbon dolphin" on 12 April 2007. In: Technical report NOU 2008, vol 8. Royal Norwegian Ministry of Justice and the Police
3. Nielsen LG (2004) Casualty report: Stevns power capsizing and foundering during anchor handling operation on 19 October 2003. In: Technical report 199940518, Danish Maritime Authority

4. Gunnu GRS, Moan T (2012) Stability assessment of anchor handling vessel during operation considering wind loads and wave induced roll motions. In: The 22nd international offshore and polar engineering conference. ISOPE, Rhodes
5. Hukkelås T (2012) How to increase the safety during anchor handling operations?. Technical report, Kongsberg Maritime AS, Kongsberg
6. Gunnu GRS, Moan T, Chen H (2010) Risk influencing factors related to capsizing of anchor handling vessels in view of the bourbon dolphin accident. In: The international conference on systems engineering in ship and offshore design. Royal Institution of Naval Architects, Bath
7. Ritchie G (2007) Practical introduction to anchor handling and supply vessel operations, 2nd edn. Clarkson Research Services Limited, London
8. Gibson V (2009) Supply ship operations, 3rd edn. La Madrila Press, Aberdeen
9. IMCA (2000) Specification for DP capability plots. International Marine Contractors Association, London
10. Gonsholt A, Nygård B (2002) Dp design studies. In: Dynamic positioning conference. Marine Technology Society, Houston
11. IMCA (2009) International guidelines for the safe operation of dynamically positioned offshore supply vessels. International Marine Contractors Association, London
12. Augusto OB, Andrade BL (2003) Anchor deployment for deep water floating offshore equipments. Ocean Eng 30(5):611–624
13. Wennersberg LAL (2009) Modeling and simulation of anchor handling vessels. Thesis, Norwegian University of Science and Technology
14. MSS, Marine systems simulator (2010) Technical report. http://www.marinecontrol.org. Accessed 15 March 2011
15. Gunnu GRS, Wu X, Moan T (2012) Anchor handling vessel behavior in horizontal plane in a uniform current field during operation. In: Choo YS, Edelson DN, Mills T (eds) The 2nd marine operations specialty symposium. Research Publishing Services, Singapore
16. SIMO project team (2012) SIMO - Theory Manual Version 4.0 rev. 1, MARINTEK, Trondheim, Norway
17. Ormberg H, Passano E (2012) RIFLEX theory manual. MARINTEK, Trondheim
18. Faltinsen OM (1990) Sea loads on ships and offshore structures. Cambridge University Press, Cambridge
19. Naciri M, Sergent E (2009) Diffraction/radiation of 135,000 m^3 storage capacity LNG carrier in shallow water: a benchmark study. In: The ASME 2009 28th international conference on ocean, offshore and arctic engineering. ASME, Honolulu
20. Wadam DNV (2010) Wave analysis by diffraction and Morison theory. In: SESAM user manual. Det Norske Veritas, Høvik
21. Blendermann W (1994) Parameter identification of wind loads on ships. J Wind Eng Ind Aerodyn 51(3):339–351
22. Ringen E, Moi S (2012) ShipX station keeping plug-in. MARINTEK, Trondheim
23. Zhou L, Moan T, Riska K, Su B (2013) Heading control for turret-moored vessel in level ice based on Kalman filter with thrust allocation. J Mar Sci Technol 1–11
24. Fossen TI (2011) Handbook of marine craft hydrodynamics and motion control. Wiley, West Sussex
25. DNV (2010) Recommended practice DNV-RP-C205, environmental conditions and environmental loads. Det Norske Veritas, Høvik
26. Rustad AM, Larsen CM, Sørensen AJ (2007) Deep water riser collision avoidance by top tension control. ASME, London
27. ISO (2005) International standard ISO 19901-1. Metocean design and operating considerations, 1st edn. In: Petroleum and natural gas industries—specific requirements for offshore structures. International Standard, Switzerland
28. DNV (2010) Offshore standard DNV-OS-E301, position mooring. Det Norske Veritas, Høvik